Harmful Algae 114 (2022) 102222

Contents lists available at ScienceDirect

Harmful Algae

journal homepage: www.elsevier.com/locate/hal

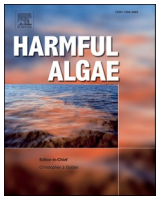

Preservation of brevetoxins in Southwest Florida coastal sediments

James Javaruski, Puspa L. Adhikari *, Joanne Muller, Michael L. Parsons

The Water School, Department of Marine and Earth Sciences, Florida Gulf Coast University, Fort Myers, FL 33965 United States

ARTICLE INFO

Edited by: Holly Bowers

Keywords:
Florida red tides
Karenia brevis
Brevetoxins
Southwest Florida
Sediment cores

ABSTRACT

Florida red tide is a natural phenomenon caused by the dinoflagellate, *Karenia brevis*. *Karenia brevis* blooms produce potent toxins (brevetoxins) that can cause neurotoxic and respiratory illness in humans and marine life. Red tides were recorded by Spanish explorers as early as the 17th century, however published red tide studies before 1940 are unavailable. Recent studies have suggested that red tide events may be becoming more frequent, intense, and longer lasting, which may be linked to modern land development and changing water quality. While the scientific record of modern red tides is relatively short, the distributions and concentrations of chemical biomarkers (e.g., brevetoxins produced by *K. brevis*) in coastal-marine sediments can potentially be used to study historic red tides. This study aims to quantify the concentration and vertical distribution of brevetoxins in coastal Southwest Florida (SWFL) sediment cores in order to determine if downcore brevetoxins may potentially be used to reconstruct historic red tide events. Sediment samples were radiometrically dated using ^{210}Pb and subsamples were analyzed utilizing liquid chromatography/triple quadrupole mass spectrometry (LC–MS/MS) for brevetoxin congeners, namely, PbTx-1, PbTx-2, PbTx-3, and PbTx-5. The ^{210}Pb–dated sediment cores represent ~60–80 years of brevetoxin accumulation and total brevetoxin (ΣPbTx) concentrations in sediment cores varied from below detection limits to 25.3 ng g^{-1} of dry sediments. Highest concentrations were found in surficial sediments (top 0–3 cm) and may indicate brevetoxin preservation from the 2017–2019 red-tide event. The down-core preservation and variability of brevetoxin indicate its potential use as a chemical biomarker to assess long-term red tide intensities and frequencies. This research is a first step towards reconstructing historic red tide events from sedimentary chemical biomarkers and may allow for future assessment of the human impacts on red tide frequency, intensity and duration.

1. Introduction

Blooms of the toxic marine dinoflagellate (*Karenia brevis*) reoccur nearly annually in the coastal regions along the Gulf of Mexico. *Karenia brevis* is well known for producing extensive algal blooms in Southwest Florida (SWFL) commonly referred to as red tides. Red tide causes significant ecological and economic loss, largely through the creation of oxygen-deficient "dead zones" and the production of potent neurotoxins (Anderson et al., 2000; Dupont et al., 2010; Morgan et al., 2007). The fragile and unarmored dinoflagellate (*K. brevis)* lyses due to wind-driven wave action, releasing neurotoxins (brevetoxins, PbTx) into the water column (Pierce et al., 1990, 2000). Once lysed, brevetoxins can be transported to the surface as droplets and subsequently aerosolized into the atmosphere when bubbles burst (Pierce et al., 1990, 2000, 2003). Water column and atmospheric (aerosolized) brevetoxins cause neurotoxic and respiratory effects to human and marine life (Baden et al., 2005; Fleming et al., 2007; Kirkpatrick et al., 2006). The aerosolized toxins affect human respiration by exacerbating asthma and inducing bronchoconstriction in otherwise healthy individuals (Fleming et al., 2007; Kirkpatrick et al., 2006). Recent studies suggest that airborne brevetoxins may be more harmful than health officials previously thought, with the toxin side effects extending beyond initial acute reactions (Backer et al., 2005; Fleming et al., 2005, 2011). Ingesting shellfish contaminated with brevetoxins may result in neurotoxic shellfish poisoning, paresthesia (the reversal of hot and cold temperature sensation), vertigo, and ataxia in humans (CDC, 2019). In marine animals such as manatees, ingestion of large amounts of brevetoxins from eating contaminated seagrass, or breathing in aerosolized toxins, can result in symptoms such as seizures that result in drowning (Domingo et al., 2001). In large blooms, brevetoxin exposure can result in substantial fish kills, depleting local fish populations (Dupont et al., 2010). As these blooms progress, the sinking and decay of dead organisms, predominantly *K. brevis* cells, leads to an increased biochemical oxygen demand (BOD), ultimately resulting in hypoxic conditions

* Corresponding author.
E-mail addresses: padhikari@fgcu.edu, puspa.adhikari@gmail.com (P.L. Adhikari).

https://doi.org/10.1016/j.hal.2022.102222
Received 6 September 2021; Received in revised form 25 February 2022; Accepted 6 March 2022
Available online 16 March 2022

(Dupont et al., 2010; Joyce, 2000). Such hypoxic waters create a positive feedback loop killing more organisms due to a lack of dissolved oxygen (Conley et al., 2009; FDEM, 2018).

Red tide events have occurred for centuries, having been recorded by Spanish explorers as early as the 17th century, with preserved written accounts from the 1840s (Ingersoll, 1881; Kusek et al., 1999; Magaña et al., 2003; Rounsefell and Nelson, 1966). Though red tides are a natural phenomenon, studies in Southwest Florida are beginning to show that they may have become more frequent, intense, and longer-lasting over the last several decades (Brand and Compton, 2007; Burns, 2008). It has been reported that *Karenia brevis* was approximately 13–18 times more abundant in 1994–2002 than in 1954–1963, though this could be due to improvements in our ability to detect blooms (Brand and Compton, 2007). In addition to a general increase in abundance, this study also noted changes in cell density. The top 22 samples (out of 2158 samples) for 1954–1963 averaged 2.5 million cells L^{-1}, while the top 33 samples (out of 3312 samples) for 1994–2002 averaged 34.7 million cells L^{-1} (Brand and Compton, 2007). Population growth and subsequent increase in nutrient runoff are considered to be the major causes of the recent increase in global harmful algal bloom (HAB) frequency, intensity, and duration (Brand and Compton, 2007; Kennish et al., 2007; Paerl and Barnard, 2020; Xu et al., 2010). The population of Florida increased from 4 to 6 million to 22 million between 1960 and 2020; however, the scientific data to correlate historic red tide events to increasing human activity are not available (Heil et al., 2014; Macrotrends, 2021).

In October of 2017, an unprecedented red tide event began in the coastal waters of SWFL and persisted through February of 2019. By August of 2018, the bloom covered approximately 150 miles of coastline, resulting in more than 2000 tons of dead fish being removed from public beaches (US Department of Commerce, 2019). In addition to the mass mortality of fish, a large number of marine mammals died. Between 2017 and 2019, 600 sea turtles, more than 200 manatees, and 204 dolphins were killed by the red tide (FWC, 2018, 2021). With many of these dead marine animals washing onshore, tourism (Florida's largest industry) was disrupted, with the direct red tide event impacts exceeding $184 million in economic losses (Court et al., 2021).

Brevetoxins produced by red tides (*K. brevis*) are lipid soluble polycyclic polyethers. This suite of toxins is broken down into two groups, Type A and Type B, based on their polyether backbones (Fig. S1). Type A consist of PbTx-1, 7, and 10 and Type B consist of PbTx 2, 3, 5, 6, 9, 11 and 12 (Ishida et al., 2004; Nakanishi, 1985). Four of the nine congeners, namely, PbTx-1, PbTx-2, PbTx-3, and PbTx-5 have been frequently reported in previous studies. Among them, PbTx-1, PbTx-2, and PbTx-3 are the most toxic forms (Pitt, 2007). Moreover, PbTx-2 is the most prevalent toxin within a *Karenia* cell and PbTx-3 is the primary brevetoxin recovered from marine aerosols that affect both marine mammals and human respiratory function (Pierce et al., 2007, 2003). In 2007, Brand and Compton reported that brevetoxins may persist in the environment longer than previously thought. Kieber et al. (2010) investigated the effects of photodegradation, oxygen levels, colored dissolved organic matter (CDOM), and trace metals on the fate of brevetoxins (PbTx-2) in seawater. PbTx-2 exhibited a half-life of approximately 3 h in surface seawater under relevant conditions; however, this degradation of PbTx-2 was not due directly to photolysis (Kieber et al., 2010). concluded that an indirect photochemical pathway, under relevant conditions (in terms of CDOM, molecular oxygen and trace metals), could be an important sink for the dissolved brevetoxins in seawater. In the absence of sunlight, degradation of PbTx-2 stops regardless of the organic matter, oxygen, or trace metal concentrations (Kieber et al., 2010). Therefore, CDOM rich coastal waters with low light penetration may exhibit long-term preservation of brevetoxins (Hardman et al., 2004).

Even though red tides have been recorded and monitored for a long time, the records tend to be relatively short and discontinuous. However, it may be possible to assess historic red tide intensities and frequencies by analyzing chemical biomarkers (i.e., brevetoxins) preserved in seafloor sediments. Brevetoxins readily sorb onto suspended particles such as fine-grained sediments and sink to the seafloor (Pierce et al., 2007). Sediment cores have been previously used to develop harmful algal bloom signatures, including other toxins, dinoflagellate cyst assemblages, and diatom valves (*Pseudo-nitzschia* spp.) (D'Silva et al., 2012; Hobbs et al., 2021; Parsons et al., 2002; Zastepa et al., 2017). In 2008, Mendoza et al. demonstrated that toxins are present in surface sediments but to date a time series record of downcore brevetoxins has not been reported. Consequently, the long-term fate of brevetoxin in SWFL coastal-marine sediments is still unknown. This research aims to quantify the concentrations, distribution, and accumulation rates of brevetoxins in shallow SWFL coastal sediments in order to determine if brevetoxins preserved in sediments can be used to reconstruct historic red tide events.

2. Materials and Methods

2.1. Site selection

Sediment cores were collected from five shallow water (0.5–1 m) coastal sites near Sanibel and in Estero Bay in SWFL (Fig. 1) for brevetoxin analysis and sediment dating. Sampling sites were selected based on the 2017–2019 red tide bloom locations and intensity as reported by the Florida Fish and Wildlife Commission (FWC, 2020). While these sites do not represent the distributions and accumulation rates of brevetoxins for the offshore West Florida Shelf, the selected sites represent general red tide accumulations for frequently affected inshore SWFL. All the sites were void of seagrass and other visible benthic macrofauna. Sampling sites were subject to tidal fluctuations but generally protected from human and boat traffic, allowing for the movement of brevetoxins into the sites but minimizing the amount of potential human sediment disturbance. Satellite views of sites can be found in the supplemental document (Fig. S2). Sites 1, 2, and 3 were directly adjacent to the Estero Bay inlets, and Site 4 was adjacent to an inlet south of Estero Bay that leads into a series of canals. Site 5 was located on the leeward side of Sanibel Island. Each site was located near a barrier island and had predominately very fine to fine-grained sandy sediments. Our sampling locations in Estero Bay (Sites 1 and 2) were near the sampling locations (BCP and BHP) from Mendoza et al. (2008).

2.2. Sample collection and preservation

At each site, two sediment cores were collected using a push corer with 7.6 cm diameter aluminum tubes and handles. The first core from each site was used for brevetoxin analysis and was sliced at 1 cm intervals for the top 5 cm, and then at 2 cm intervals to a total depth of 11 cm. The second core from each site was used for ^{210}Pb-based sediment dating and was sliced at 1 cm intervals to 11 cm, followed by 2 cm intervals until a depth of 30 cm. All of the extruded sediment samples were collected in amber jars and then frozen at −20 °C until lab analysis (Fig. S3).

2.3. Laboratory analyses

2.3.1. Sediment dating

The sample preparation, radioactive counting, and modeling for ^{210}Pb–based sediment dating have been previously described by Adhikari et al. (2016). Briefly, the sediment samples (with known volume in graduated vials) were weighed to determine the wet weight followed by drying at 60 °C for 24 hr. The weights were then recorded before being placed in the oven for an additional 24 hr. Samples were then weighed again upon removal and the difference measured until a constant weight, to ensure that the samples were completely dry (Martin and Muller, 2021). Using dry weight and volume, sediment density was calculated. Following this, the aliquots were ground with a mortar and

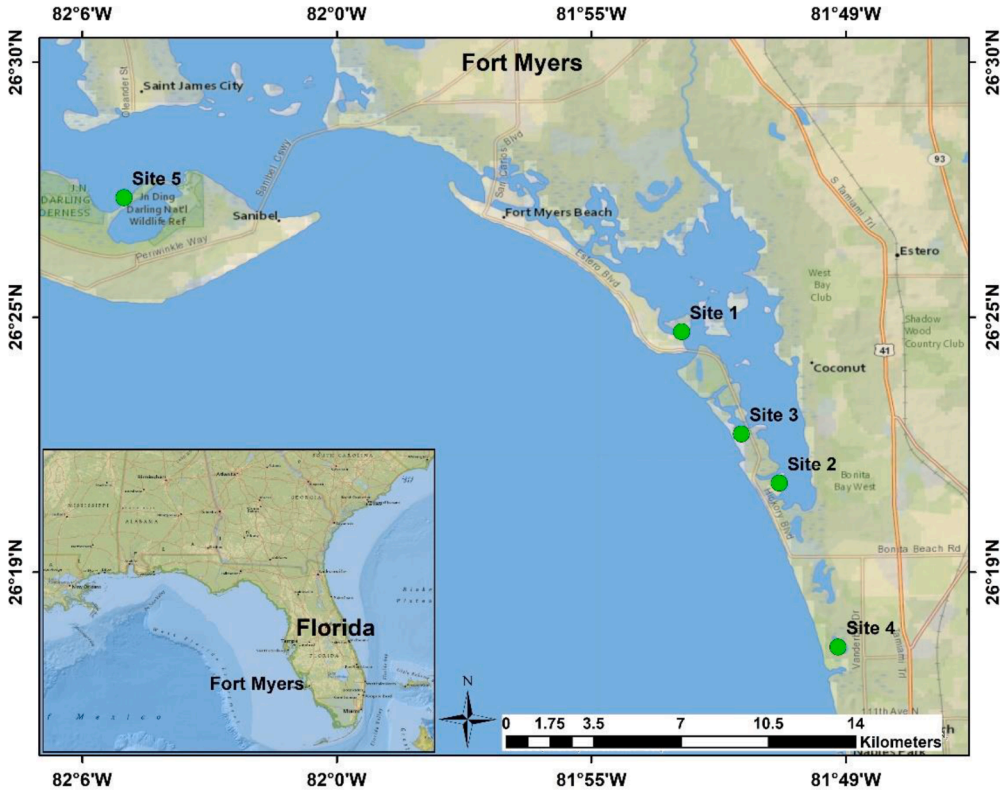

Fig. 1. Sampling locations in Southwest Florida. Sediment cores were collected from three sites in Estero Bay, one site south of Estero Bay, and one site behind Sanibel Island in Southwest Florida.

pestle. Approximately 28 to 32 g of dried ground sediments were placed into counting vials of known geometry and sealed (using epoxy) before measuring for ^{210}Pb and ^{226}Ra (via ^{214}Pb) through direct counting using SAGe High-Purity Germanium Detectors (Adhikari et al., 2016). All activities were decay corrected to the midpoint of sample collection. Unsupported ^{210}Pb ($^{210}Pb_{ex}$) was calculated as the difference between the measured total ^{210}Pb at 46.5 keV and the estimate of the supported ^{210}Pb activity given by its parent nuclide ^{214}Pb at 351 keV [$^{210}Pb_{ex} = {}^{210}Pb_{tot} - {}^{214}Pb$]. The sedimentation and sediment accumulation rates were calculated using the CRS (constant rate of supply) model. The CRS model allows sedimentation rates to vary over time and is thus more applicable for shallow coastal areas (Adhikari et al., 2016; Appleby and Oldfield, 1992; De Souza et al., 2012; Lubis, 2006) like Southwest Florida coastal-marine environments where large anthropogenic activities can alter the sediment loads. Errors represent counting statistics (Adhikari et al., 2016). The details about radioactive counting using germanium gamma detectors and modeling using CRS are presented in the Supplemental Document (ST: Sediment Dating).

2.3.2. Brevetoxin extraction and analysis

The sample extraction and analysis was performed using a previously described method (Pierce et al., 2003; Mendoza et al., 2008), with slight modification. Briefly, before the extraction of brevetoxins, the frozen sediments samples were thawed overnight in a refrigerator and homogenized by mixing with a solvent-cleaned steel stirring spoon. Aliquots of approximately 30 g of wet sediments from each layer were placed into a pre-cleaned 250 mL beaker and mixed with solvent-cleaned anhydrous sodium sulfate to absorb moisture in the sediments. The dry sediment/sodium sulfate mixture was transferred to a solvent-cleaned cellulose extraction thimble. The samples were then extracted with acetone for 24 hr using Soxhlets (Guerin, 1999; Pierce et al., 2003). The solvent (acetone) was evaporated to dryness using a Bucchi rotary evaporation system and then the dried sample extracts were dissolved in methanol for solvent exchange. This was followed by further concentration of the sample extracts using nitrogen blow-down to a final volume of 5 mL. The sample extracts were then transferred into a 5 mL amber vial, capped, and stored at −20 °C until lab analysis (Pierce et al., 2003).

The sample extracts were analyzed for brevetoxins using a Thermo Electron Quantum Access Liquid Chromatography/Tandem Mass Spectrometry (LC-MS/MS) at Mote Marine Laboratory, Sarasota, Florida. The LC consists of an Accela Ultra-High-Performance Liquid Chromatography (UHPLC) pumping system coupled with the Accela Autosampler and Degasser. Mass spectral detection was obtained using a Quantum Access triple quadrupole (MS/MS) mass spectrometer. The analytical column was a Phenomenex Kinetex 2.6 μm particle size with dimensions of 100 × 2.1 mm. The solvent gradient was composed of acetonitrile with 0.1% formic acid (A) and HPLC water with 0.1% formic acid (B) with initial conditions of 50:50 (A:B) for 10 min to 95:5 for 5 min and a holdback to 50:50 for 5 min for a total sample run time of 20 min at a flow rate of 200 μl min^{-1}. The reagent grade (>99.9%) acetone and methanol used in this study were purchased from Sigma-Aldrich. The A.C.S. certified sodium sulfate (anhydrous, 10–60 mesh) was purchased through Fisher Scientific, Waltham, MA. Ultra-High Purity Nitrogen (99.99%) was obtained from Matheson Gas, Fort Myers, Florida. PbTx-1, −2, −3 and −5 standards for the calibration of the LC-MS/MS were obtained from the University of North Carolina Wilmington (UNCW), Center for Marine Science/MARBIONC. The sum of the four congeners analyzed in this study, namely, PbTx-1, PbTx-2, PbTx-3, and PbTx-5, are presented as ∑PbTx. The reported concentrations of brevetoxins are in nanograms of toxin per gram of dry sediments (ng g^{-1} dry sediments). The detection limits for each congener were PbTx-1 0.323 ng g^{-1}, PbTx-2 0.170 ng g^{-1}, PbTx-3 0.028 ng g^{-1} and PbTx2-CA 0.239 ng g^{-1}. Brevetoxin concentrations are not recovery-corrected as surrogate standards (e.g., PbTx-9) were not available.

2.3.3. Grain size analysis

Studies have demonstrated that marine contaminants sorb more

efficiently to the finer grain fraction of sediments, yet other work has shown little correlation between lipophilic marine phycotoxins and grain size (Guven and Akinci, 2013; Liu et al., 2019). To account for this, grain size data was collected and compared to toxin concentrations. Subsamples (10 g) of dried sediments (from the core sliced for ^{210}Pb analysis) were placed into plastic weigh boats and dried for 24 hr at 60 °C. They were then stored in sealed sample bags until further analysis. Each sample bag was massaged for 20 s to disaggregate sediments, then shaken for another 20 s to achieve a homogenized mixture. A representative sample from this homogenized sediment was weighed and then combusted at 450 °C in a muffle furnace for 12 hr to burn off organic matter. The samples were then weighed immediately after they were removed from the furnace to determine the total organic carbon (Schumacher, 2002).

Grain size analysis was performed using a Malvern Mastersizer 3000 with a HydroEV attachment that has minimum and maximum grain size detection limits of 0.01–2500 μm. A 2 g aliquot was taken from the homogenized and combusted sediment sub-sample and sieved through a 2000 μm sieve. The weight of any grains above this size was recorded. The Mastersizer was instructed to sample for 30 s using the red laser (632.8 nm) and an additional 30 s using the blue laser (470 nm). Five replicate measurements were taken to calculate an average. The grain sizes were binned in increments of 0.25 Phi ranging from 11 Phi (0.49 μm) to −1 Phi (2000 μm).

3. Results

3.1. ^{210}Pb-based sediment dating and sediment accumulation rates

The activities of excess ^{210}Pb at all sampling locations were low, even after running each sample in the germanium detector for ~3 days. Previous sedimentary studies from the SWFL region showed ^{210}Pb sediment dating in this region to be challenging; however, in this study we were able to date cores from Sites 1, 3, and 4 (Fig. 2). Sediment accumulation rates are 0.04–1.11, 0.03–0.78, and 0.03–0.65 g cm^{-2} yr^{-1} for Sites 1, 3, and 4 respectively (Tables 1, and S1). Another study by (Savarese et al., 2004) also showed similar sedimentation accumulation rates (0.25 g cm^{-2} yr^{-1}) in this area, corroborating our results.

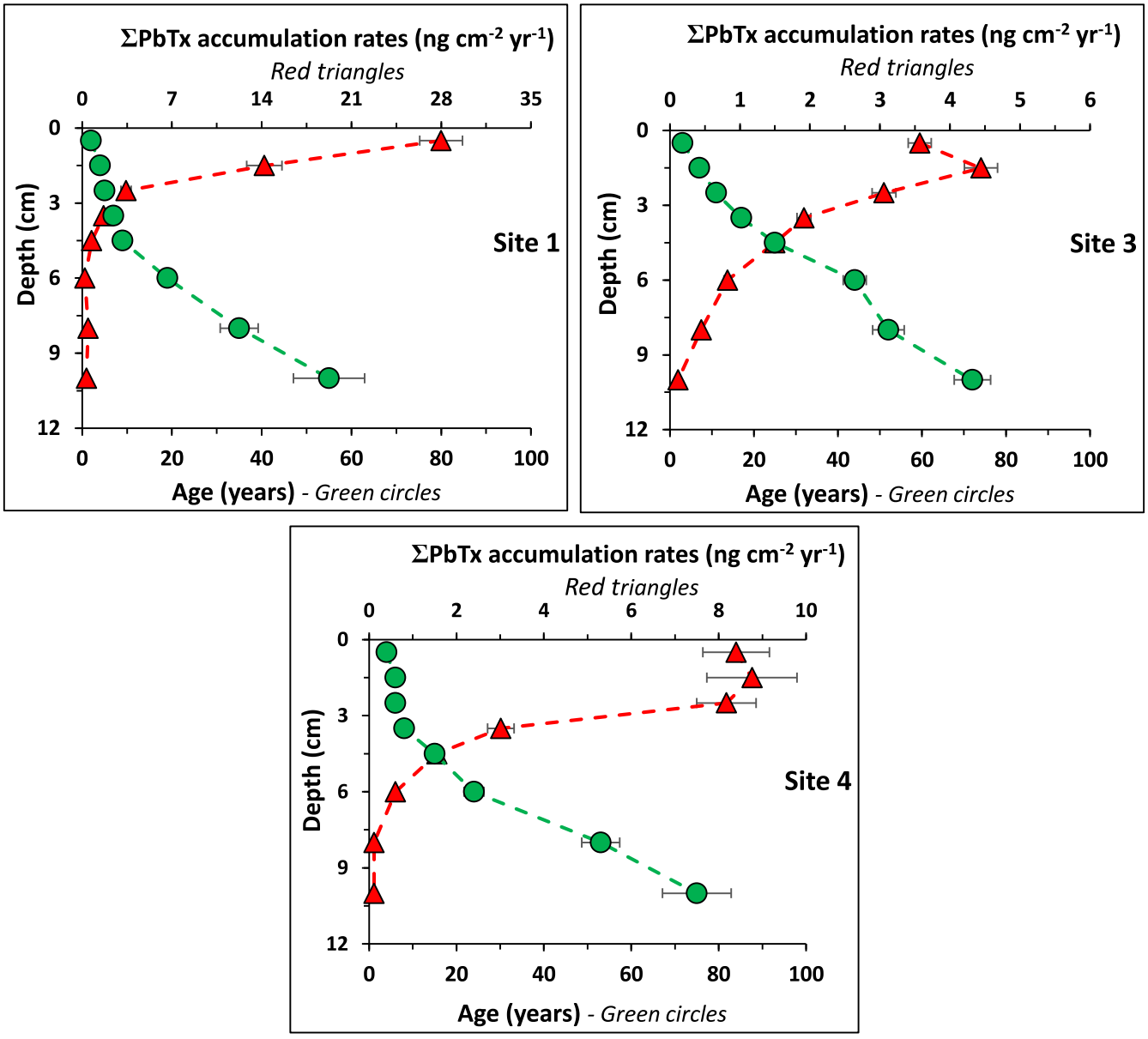

Fig. 2. The age of the sediments (years) and total brevetoxins (∑PbTx) accumulation rates (ng cm^{-2} yr^{-1}) for sediment cores collected from Site 1, Site 3, and Site 4. The upper x-axis represents sediment accumulation rate and the lower x-axis represent sediment age.

Dating estimates from Site 1 indicate that it is representative of ~55 years of sedimentation. Dating estimates from Site 3 indicate that the top 1–3 cm of sediments tends to be modern in age, and the top 11 cm of the sediment represents ~72 years of sedimentation, and consequently ~72 years of brevetoxin accumulation. Dating estimates from Site 4 indicate that it is representative of ~75 years of sedimentation. Site 1 demonstrated the highest average sediment accumulation rate (0.04–1.11 g^{-1} cm^{-2} yr^{-1}) followed by Site 4 (0.03–0.65 g^{-1} cm^{-2} yr^{-1}) and Site 3 (0.03–0.78 g^{-1} cm^{-2} yr^{-1}).

3.2. Concentrations and accumulation of brevetoxins

The concentrations of total brevetoxins (∑PbTx), the sum of PbTx-1, PbTx-2, PbTx-3, and PbTx-5 congeners, varied from 0.3 to 25.3 ng g^{-1} of dry sediments (Fig. 3). Generally, sediment cores exhibited ∑PbTx peaks at different depths (Fig. 3) however, some similarities can be seen. For example, all sites except Site 3 noted highest ∑PbTx in the top 0–3 cm. At Site 3, highest concentrations are noted between 2 and 5 cm. Site 1 exhibited an additional smaller peak in ∑PbTx at a depth of 9–11 cm (Fig. 3).

The concentrations of individual brevetoxin congeners varied

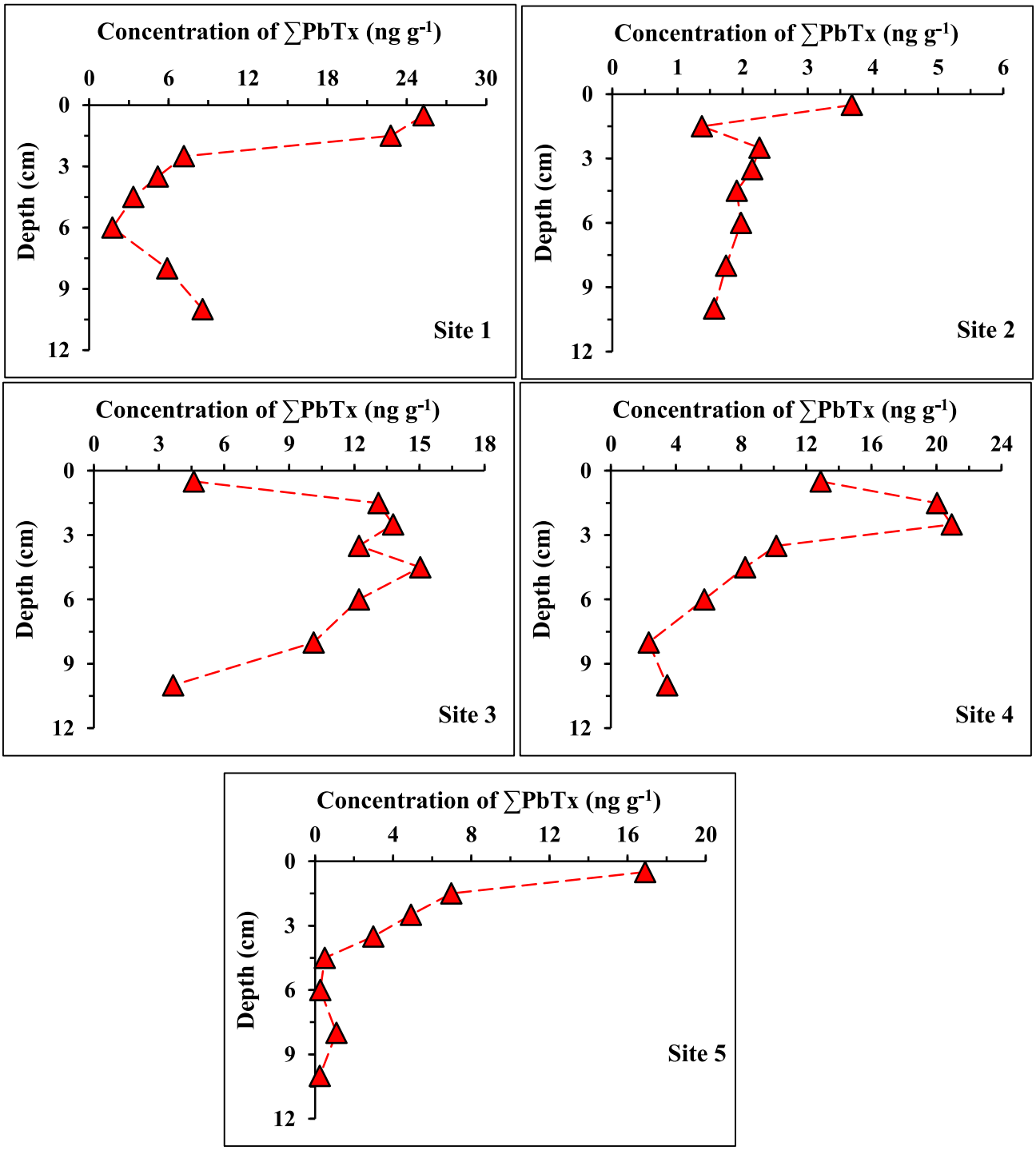

Fig. 3. Concentrations of total brevetoxins (∑PbTx) in ng g^{-1} of dry weight of sediments (summation of all congeners analyzed in this study) at each depth.

between ND and 13.5 ng g^{-1} throughout the sampling locations (Fig. 4). Out of the four congeners analyzed, two congeners (PbTx-2 and PbTx-3) were detected at all sites (Fig. 4). PbTx-3 was detected in all cores and at all depths. PbTx-2 was absent only in the deeper sediments (4–11 cm) at Site 5. Among the four brevetoxin congeners, PbTx-2 showed the highest concentrations (0.7–13.5 ng g^{-1}) in four out of five study sites (Fig. 5). PbTx-2 contributed 39% to 69% of the total brevetoxins at those sites (Fig. 5). PbTx-5 had the lowest concentrations, with a range of 0–3.8 (avg. 0.83) ng g^{-1} dry sediment and contributed 0–48% (avg 8%) of the ∑PbTx.

At Sites 1, 3, and 4, PbTx-2 showed higher concentrations (1.64–13.5 ng g^{-1}) in the top 5 cm of the sediments compared to underlying sediments. At these sites, PbTx-1 and PbTx-3 were also in higher concentrations, reaching up to 7.8 and 6.7 ng g^{-1} dry sediment, respectively (Fig. 4, Table S2). As seen with ∑PbTx the individual congeners at Site 2 were in low concentrations and PbTx-1 is completely absent. At Site 5, concentrations of individual congeners are also relatively low, in comparison to Sites 1, 3, and 4, however some peaks in PbTx-2, PbTx-3 and PbTx-5 are seen in the upper sediments (0–4 cm). Similar to Site 2, PbTx-1 is completely absent at Site 5.

The ^{210}Pb-based sediment accumulation rate was used to estimate total brevetoxin accumulation rates with the following equation.

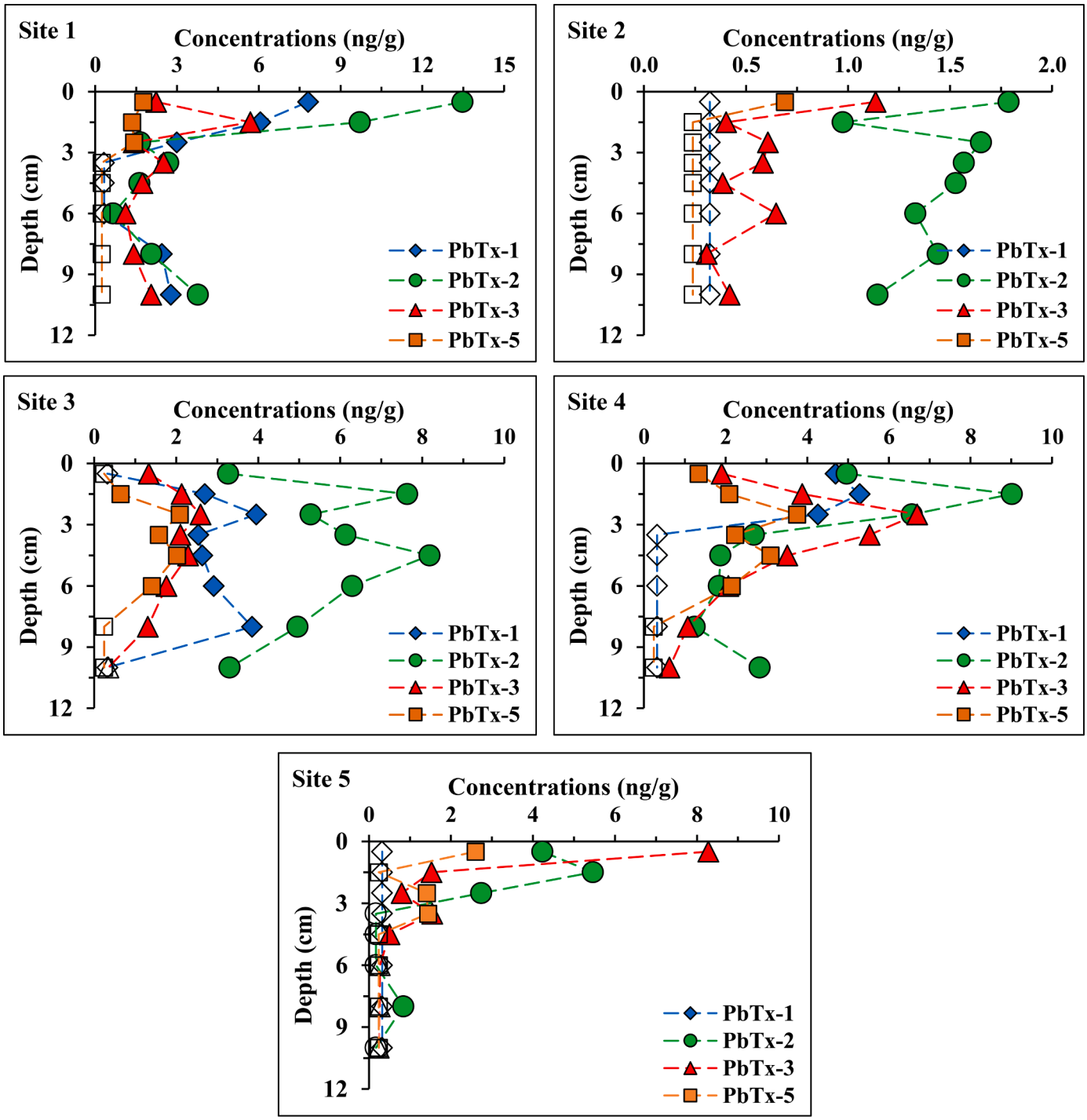

Fig. 4. The concentrations of the individual brevetoxin congeners (PbTx-1, PbTx-2, PbTx-3, PbTx-5) measured in each core. The open markers for each congener represent the concentration of congeners below detection limits.

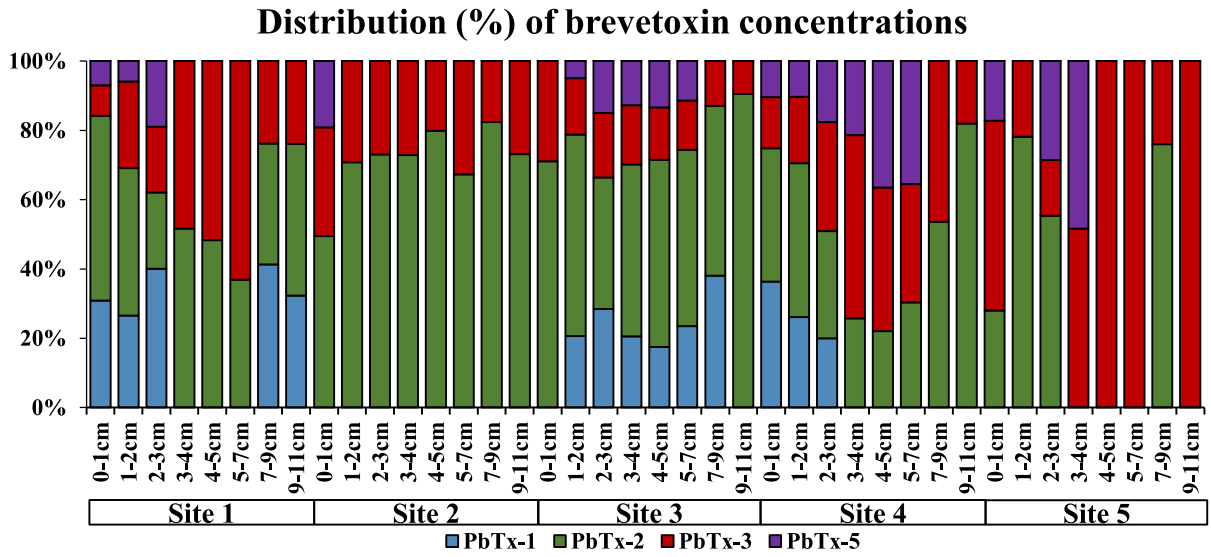

Fig. 5. The percentage of each congener of brevetoxin (PbTx-1, PbTx-2, PbTx-3, PbTx-5) found at each depth at each site. The values (%) on the y-axis represent the contribution of each congener to the total brevetoxin concentrations.

$$\sum PbTx \text{ accumulation rates } = C_i \times A_i$$

Where C_i (ng g^{-1}) and A_i (g cm^{-2} y^{-1}) represent ∑PbTx concentrations and sediment accumulation rates of each segment, respectively.

The accumulation rates of ∑PbTx at Sites 1, 3, and 4 were found to vary between 0.3–28 (avg: 6.1), 0.1–4.4 (avg: 2.0), and 0.1–8.8 (avg: 3.8) ng cm^{-2} $year^{-1}$ respectively (Table 1). Site 1 exhibited the higher brevetoxin accumulation rates followed by Sites 3 and 4 (Fig. 2). The top 4 cm of all cores showed higher brevetoxin accumulation rates than the underlying sediments (Fig. 2).

Table 1
The age (years), sediment accumulation rates (g cm^{-2} yr^{-1}), and ∑PbTx accumulation rates (ng cm^{-2} yr^{-1}) at sampling Sites 1, 3, and 4.

	Depth (cm)	ΣPbTx concentrations (ng g^{-1})	Estimated age (yr)	Sed. accumulation rates (g cm^{-2} yr^{-1})	∑PbTx accumulation rates (ng cm^{-2} yr^{-1})
Site 1	0–1	25.3	2	1.11	28
	1–2	22.8	4	0.62	14.2
	2–3	7.2	5	0.48	3.4
	3–4	5.2	7	0.32	1.7
	4–5	3.3	9	0.22	0.7
	5–7	1.8	19	0.12	0.2
	7–9	5.9	35	0.08	0.5
	9–11	8.6	55	0.04	0.3
Site 3	0–1	4.6	3	0.78	3.6
	1–2	13.1	7	0.34	4.4
	2–3	13.8	11	0.22	3.1
	3–4	12.2	17	0.16	1.9
	4–5	15.0	25	0.10	1.5
	5–7	12.2	44	0.07	0.8
	7–9	10.1	52	0.04	0.4
	9–11	3.7	72	0.03	0.1
Site 4	0–1	12.9	4	0.65	8.4
	1–2	20.0	6	0.44	8.8
	2–3	20.9	6	0.39	8.2
	3–4	10.2	8	0.30	3
	4–5	8.2	15	0.19	1.6
	5–7	5.7	24	0.11	0.6
	7–9	2.3	53	0.05	0.1
	9–11	3.5	75	0.03	0.1

3.3. Sediment characteristics and correlation with brevetoxins

The sediments were mainly composed of very fine to medium sands (0.0625–0.5 mm, < 4 Phi) which contributed 41.19–69.61% of the total grain size distribution. The grain size across sampling locations and along the core depths was not normally distributed (Fig. S4). Site 5 had nearly no detectable clay-sized (< 0.0039 mm, > 8.0 Phi) particles in the core (<1%). Similarly, Site 4 had no detectable clay-sized particles. In contrast, Site 3 had the highest concentration of clay-sized particles, with a range of 0.42 to 1.67% (avg: 1.07%). Site 2 had a minimum of 0.07% and a maximum of 0.6% (avg: 0.11%) of clay-sized grains. Site 1 had a minimum of 0.01% and a maximum of 0.5% (avg: 0.09%) of clay-sized grains. Silt-sized grains were more common, with a range of 0.18–16.86% (avg: 4.4%) (Fig. 6, Table S2). Across all sites, the concentration of clays (> 8.0 Phi) was minimal at each site, ranging from 0 to 1.67% (avg: 0.25%). The concentrations of silts (8.0 Phi > x > 4.0 Phi) was higher ranging from 0.18 to 16.86% (avg: 4.4%).

The total organic carbon (TOC) ranged from 0.5 to 13.4% across all sites (avg: 2.4%). There were four TOC peaks, one at Site 3 at 3–4 cm, Site 4 at 0–1 cm and 4–5 cm, and one at Site 5 at 0–1 cm (Fig. 7). If we discount for these four outliers, the range was generally 0.5 to 3.4% (avg: 1.7%). Concentrations of the total, as well as individual brevetoxins, did not show a significant correlation with sediment grain size (Fig. 6). Similarly, the concentrations of total brevetoxin were not significantly correlated with organic carbon, except for Site 5 (p<0.0005) (Fig. 7). The low concentrations of TOC and fine-grained sediments create difficulties in determining the influence of grain-size and TOC on brevetoxin accumulation in sediments from this study (Baumard et al., 2001).

4. Discussion

4.1. ^{210}Pb-based sedimentation rates

As reported in previous studies, low excess ^{210}Pb is typical of sediments in this region of Southwest Florida (Jenkins, 2018; Martin and Muller, 2021; Savarese et al., 2004). It is due in part to the composition and grain size of sediments and the lower sedimentation rates, unlike other Gulf of Mexico coastal regions, such as the Mississippi River delta. ^{210}Pb adsorbs more readily to organic-rich fine particles with higher surface areas, leading to higher excess ^{210}Pb in sediments that have a higher concentration of fine-grained particles (Appleby and Oldfield,

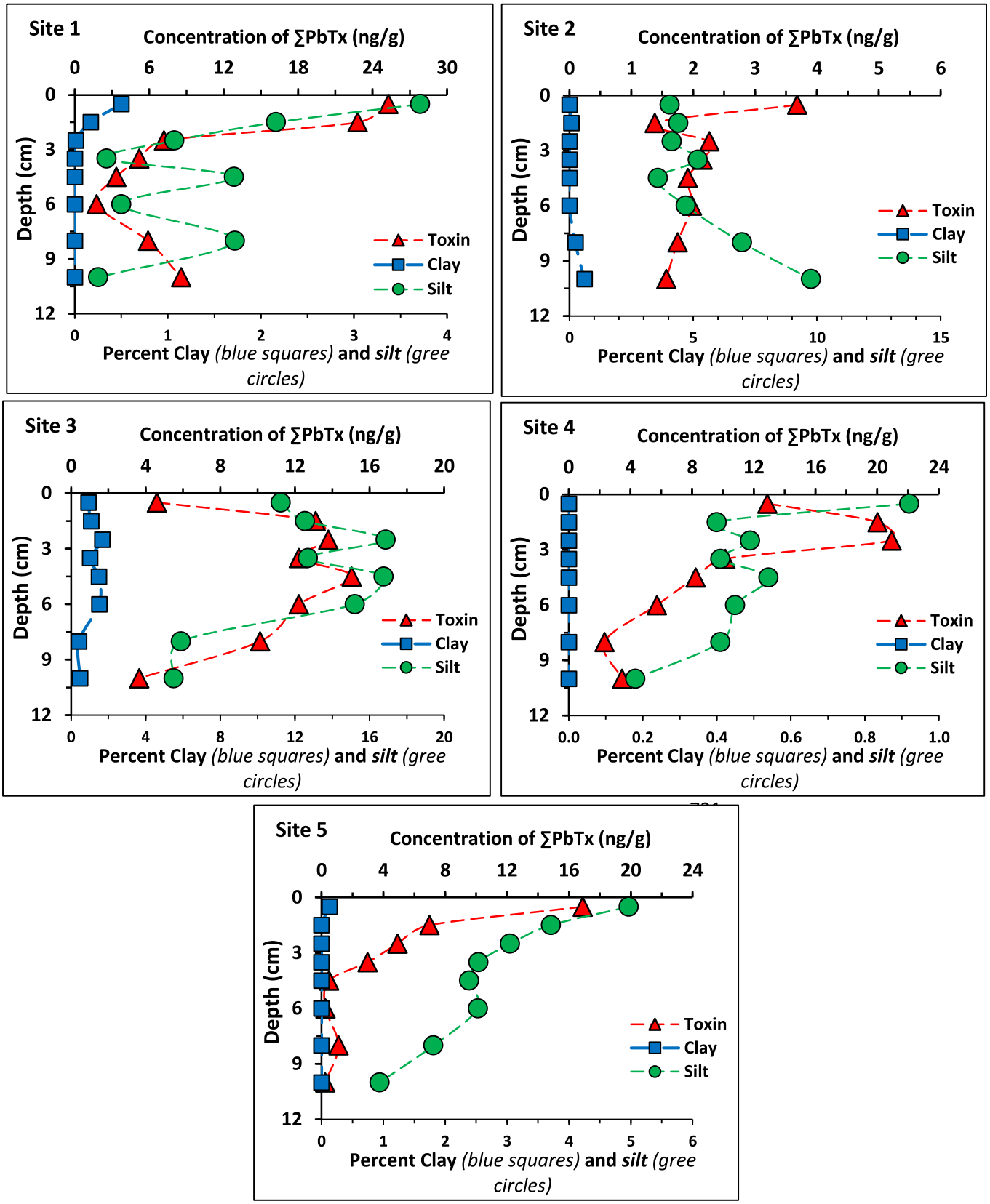

Fig. 6. The concentration of total brevetoxin (∑PbTx) plotted against the percent of clays (green squares) and silts (blue circles) at each site. The top x-axis represents the concentration of toxin (ng g^{-1} of dry weight of sediments), and the bottom x-axis is representative of the percent of clay and silts in the sediments.

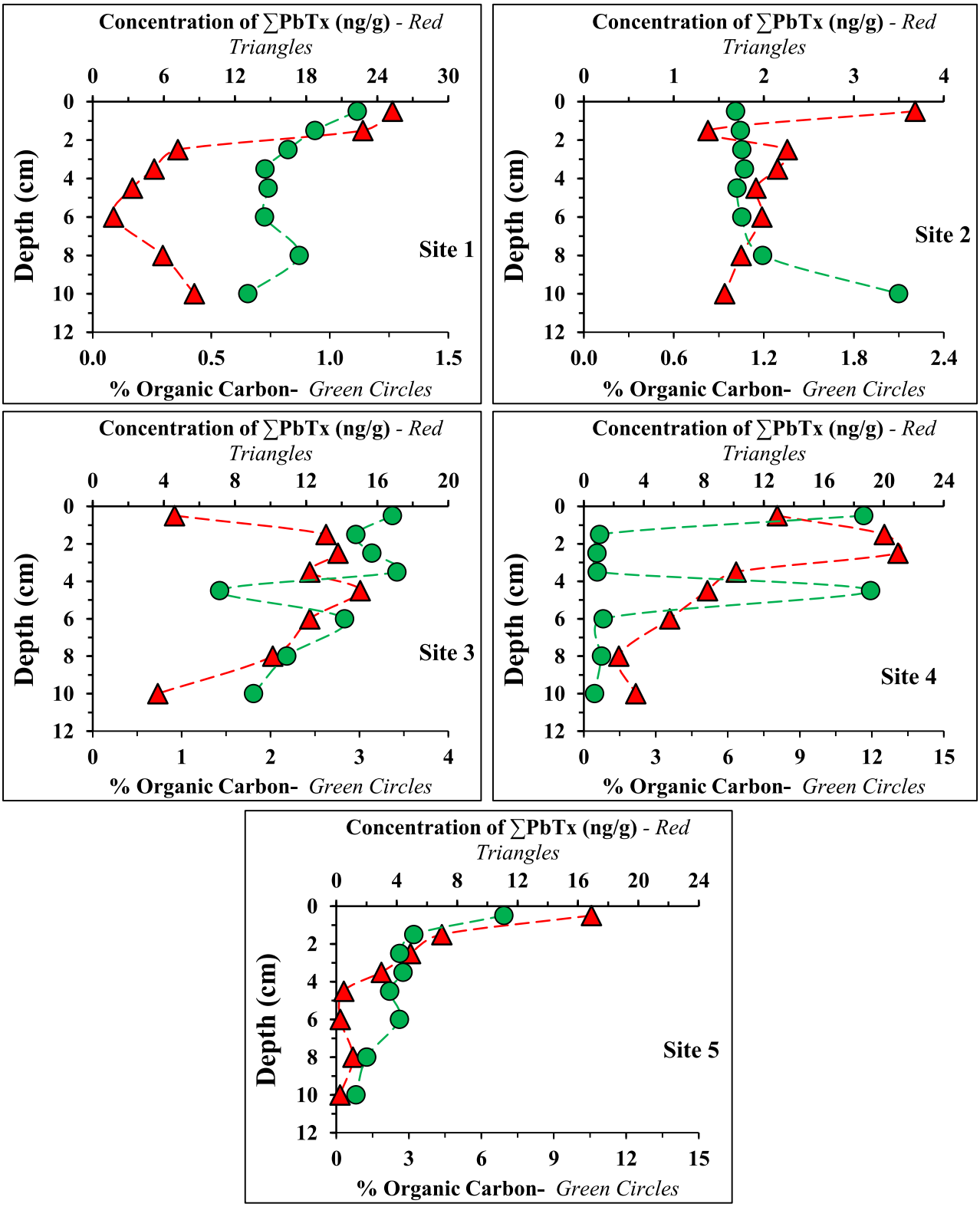

Fig. 7. The concentration of total brevetoxins (∑PbTx), in ng g^{-1} of dry sediments, in relation to total organic carbon (% organic carbon).

1978; He and Walling, 1996; Singleton et al., 2017). Generally, SWFL coastal sediments, and specifically the sample sites for this study, are mostly composed of quartz silt and sand-sized sediments (Fig. S4). As a result, the cores had relatively low excess ^{210}Pb activities (Table 1), which is the reason why we were able to date only three out of five cores (Sites 1, 3, and 4) in this study. While the sampling locations in back-barrier islands were generally protected, potential mixing/bioturbation cannot be ignored, which affects excess ^{210}Pb activities and the sediment dating. Highest sediment accumulation rates are noted at Site 1, which may be due to its location by a major tidal inlet, receiving sediment from both the Gulf of Mexico and the nearby Estero River (Fig. S2). Sediment accumulation rates are lowest at Site 4, which

may be due to its protected nature, far away from tidal inlets (Fig. S2).

4.2. Downcore concentrations and accumulation of brevetoxins

General trends are noted in the downcore concentrations of brevetoxin congeners across sites and age (Figs. 4 and 8). The PbTx-2 was detected in all sites (Fig. 4). This might be expected since PbTx-2 is the most prevalent brevetoxin in the *K. brevis* cell (Pierce et al., 2007). PbTx-3 is the second most dominant congener after PbTx-2 at Sites 1, 2 and 3. In fact, these two congeners represent 48% and 33% of the total toxin at each site, respectively (Fig. 5). As blooms age and older cells break down, the concentrations of PbTx-2 tend to decrease, however research shows that this is in part due to the conversion of PbTx-2 to PbTx-3 (Pierce et al., 2007; Poli et al., 2000). This is due to the cells degrading and releasing their contents into the water column as they are exposed to enzymatic activity. In this case, we might expect PbTx-2 concentrations to be highest, but then PbTx-3 concentrations to also be high due to some initial breakdown of cells in the water column before deposition. We also see relatively low concentrations of PbTx-5 at all sites (averaging 0.75 ng g^{-1}) while other congeners are typically double to triple of these PbTx-5 concentrations (PbTx-1, PbTx-2, and PbTx-3 averaging 1.37, 3.41 and 1.88 ng g^{-1} respectively). As PbTx-2 and PbTx-3 are the primary congeners within *K. brevis* cells and marine waters, lower quantities of PbTx-5 and PbTx-1 are to be expected (Pierce et al., 2005). Consequently, PbTx-5 is not generally addressed by red tide studies, generally making up a smaller, nearly insignificant fraction of toxin produced by *K. brevis* (Shea, 1997).

In 2008, Mendoza et al. detected brevetoxins in surface sediments taken from Estero Bay. They used homogenized surface grab samples; therefore, they did not report vertical profiles of brevetoxins in the sediments. We note slightly higher concentrations of total brevetoxins (0.13–12.91 ng g^{-1}) than those values (0.8–9.7 ng g^{-1}) previously reported by Mendoza et al. (2008). The brevetoxin congeners also showed similar trends, with generally higher concentrations in the present study compared to Mendoza et al. (2008). Mendoza et al. (2008) collected their samples in 2006 and our samples were collected in 2019, thus, the higher concentrations of ∑PbTx in the sediments from our study sites may indicate additional deposition of toxins during the 2017–2019 red tide event.

We also noted increased toxin concentrations with increased sediment accumulation rates. For example, at Sites 1 and 4, overall toxin concentrations and sediment accumulation rates have positive correlations R^2=0.85 ($P = 0.07$) and R^2=0.72 (P<0.03)) respectively (Fig. S5). This might be expected considering that a bloom event would likely increase water column productivity and therefore fluxes to the seafloor (Gobler and Sañudo-Wilhelmy, 2003). Highest ∑PbTx are noted in the top 0–3 cm at sites 1, 2, 4, and 5 (Fig. 3). At Site 3, highest concentrations are noted between 2 and 5 cm. At Site 1, the upper 2 cm extend ~4 years into the past (~2017–2021) demonstrating a clear peak of 28 ng g^{-1} dry sediment during that period. If we apply similar sedimentation rates (from Sites 1, 3 & 4) to undated Sites 2 and 5, similar brevetoxin accumulation in the top 2 cm is noted. This may suggest deposition during the 2017–2019 red tide event. Interestingly, some cores show additional peaks further downcore such as at 11 cm at Site 1 (Fig. 4, Fig. 8). Sites 4 and 5 also showed smaller peaks at 11 and 9 cm respectively. This may indicate older, historic red tide events preserved in the sedimentary record. The toxin peak noted at 11 cm at Site 1, which was deposited approximately 60 years ago (calculated from ^{210}Pb dates), may potentially correlate to a historic red tide event that took place in 1953. This event was the longest single red-tide episode recorded at that time and persisted for at least 18 months along the Florida Gulf Coast (Feinstein et al., 1955).

The presence of detectable levels of brevetoxin congeners at all sites and all depths indicates that brevetoxins (e.g., PbTx-2 and PbTx-3) are stable enough to accumulate and be preserved in sediment over time (Fig. 4). Such downcore preservation of brevetoxin congeners indicate that brevetoxins in sediments are promising biomarkers for past red tide events. This is a first step in correlating known red tide events, such as the 2017–2019 bloom, with sedimentary brevetoxin concentrations downcore. We analyzed downcore toxin concentrations to 11 cm only; thus, future studies on longer, higher resolution cores are needed to determine the viability of downcore studies in reconstructing historic red tide events. For example, Zastepa et al. (2017) showed a large increase in the concentration of microcystins since the 1985 using 0.5 cm intervals. Thus, higher resolution sampling may allow for better tracking of brevetoxin peaks in the sedimentary record.

4.3. Other potential factors affecting brevetoxin concentrations

Not all total brevetoxin (∑PbTx) profiles, nor individual brevetoxin

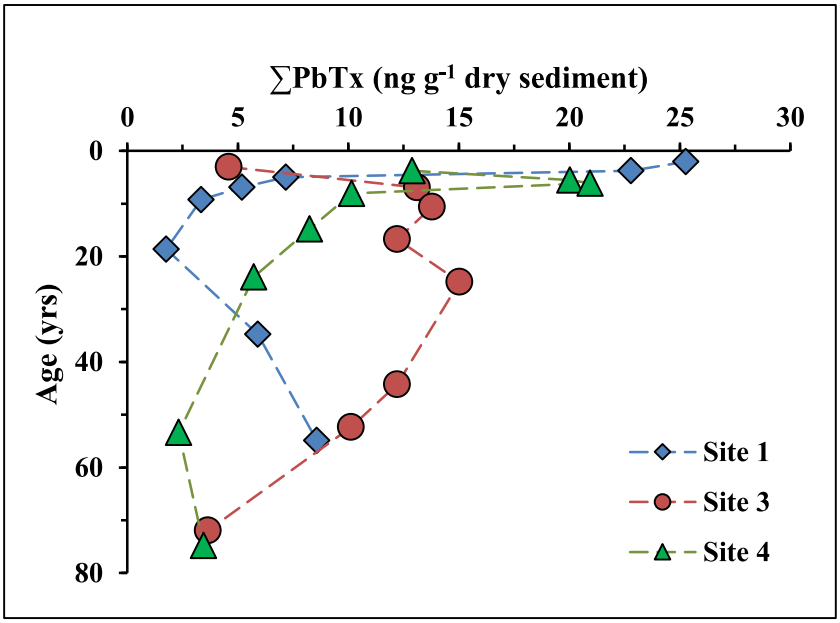

Fig. 8. Total brevetoxins (∑PbTx) concentrations (ng g^{-1}) plotted against age of the sediments for Sites 1, 3 and 4.

congener profiles, look the same across all five-field sites. This indicates that either historic red tide exposure was not the same at all sites, and/or post-depositional processes may be at play. Most likely, the brevetoxin concentrations observed at our field sites were affected by more than one environmental factor. These may include: 1) site exposure to *K. brevis* blooms; 2) water clarity; 3) diagenesis, and 4) brevetoxin post-depositional resuspension. While all of our sites are located behind barrier islands, some sites are comparatively less protected than others (Fig. S2). In addition, sites that are located behind barrier islands are adjacent to tidal inlets, thus, they may experience increased exposure to offshore red tide toxins brought by tidal currents. As tidal currents move through inlets during rising tides, the offshore and coastal blooms can be transported into the estuary (Figueiras et al., 2006). This may explain the higher brevetoxin concentrations observed at Sites 1, 3 and 4 (Fig. 3) as these sites are close to tidal inlets (Figs. 1 and S2). The relatively low concentrations of brevetoxins observed at Site 2 may be due to its greater distance from tidal inlets (Figs. 1 and S2).

Physical attributes of water such as clarity can have an effect on harmful algal bloom formation and toxin preservation (Donaghay and Osborn, 1997; Huisman et al., 1999). Before burial in the seafloor, brevetoxins that are sensitive to light undergo photodegradation. After 24 hr under natural sunlight in a laboratory, Hardman et al. (2004) reported that PbTx-2 concentrations were reduced by 35%. In the darkness, PbTx-2 was shown to be very stable, exhibiting only 3% degradation after 24 hr (Hardman et al., 2004). The darker nearshore waters of SWFL have high concentrations of tannins, which cause significant light attenuation (Ott et al., 2006). Therefore, in SWFL coastal waters, with an average Secchi depth of 1.1 m, the photodegradation of the brevetoxins is likely to be minimal (Hardman et al., 2004). This may allow for increased sorption of brevetoxins onto suspended sediments and the subsequent increase in vertical flux of brevetoxins to the seafloor where they can be preserved (Mendoza et al., 2008). At Site 5, toxins may have been more susceptible to photodegradation (even once settled on the seafloor) due to the shallower water depth and higher transparency (Secchi disk completely visible at the bottom). Lower brevetoxin concentrations at Site 5 may also be due to site exposure, due to the adjacent boat channel and higher wave energy.

Diagenesis could also influence sedimentary toxin accumulation. However, to date no published studies examine the effects of sedimentary brevetoxin diagenesis. Thus, more work on brevetoxin diagenesis is needed. As discussed above, cores taken for this research were intentionally sourced from protected back-barrier sites and indicate preservation of brevetoxin in sediments as deep as 11 cm (~60–80 years). However, it is worth noting that less protected, open nearshore and offshore locations, may be susceptible to resuspension events, which could potentially release sedimentary brevetoxins back to the overlying water column (Roberts, 2012). Resuspension could be caused by sediment entrainment from strong tidal flows or storms (Latimer et al., 1999). Storm events, such as hurricanes, can produce waves that quickly resuspend sediments. Previous studies have shown that tropical storm-generated currents are capable of resuspending sediments as deep as 100 m below the surface and translocating them over many kilometers (Dickey et al., 1998; Flaherty and Landsberg, 2011; Xu et al., 2016). Perkins (2019) found that Tropical Storm Gordon (September of 2018) may have intensified the SWFL 2017–2019 red tide event. Studies from as far back as the 1800s have shown that red tides are often intensified directly after hurricanes (Hu et al., 2006; Ingersoll, 1881). Therefore, if the research goal is to reconstruct brevetoxin back through time we argue that site selection is key (protected sites).

5. Conclusions

The primary goal of this research was to determine the longevity and preservation of brevetoxins in the sediment record and to explore whether brevetoxins preserved in sediments can be used to reconstruct historic red tide events. We found that brevetoxins were preserved in the protected back-barrier sediments of SWFL going back as far as 60–80 years (concentrations ranged from 0.2 to 25.3 ng g^{-1} of dry sediments). We found highest brevetoxin concentrations in uppermost core sediments (0–3 cm) perhaps indicating the recent 2017–2019 red tide bloom. We also note additional peaks downcore that may be correlated with older historic red tide blooms. This study is a first step in red tide event reconstruction using sediment cores. Future studies on longer, higher resolution cores may provide more detailed evidence of historic red tide intensity and frequency through time. Future studies should be cognizant of site selection as this research found best preservation in protected back-barrier sediments.

Declaration of Competing Interest

The authors declare that they have no known competing financial interests or personal relationships that could have appeared to influence the work reported in this paper.

Acknowledgments

We would like to thank Florida Gulf Coast University (FGCU) Scholarship Research Capital Venture Fund for supporting this research. Special thanks to Dr. Richard Pierce and Samantha Harlow at Mote Marine Laboratory for Brevetoxin analysis. The Small Anode Germanium Gamma Well Detector (SAGe) used for sediment dating at FGCU was funded through a National Science Foundation Major Research Instrumentation (NSF MRI) program (Award Number 1919813). Some of the radioactive analysis was conducted at Louisiana State University (LSU). Especial thanks to Drs. Kanchan Maiti and Wokil Bam for their help in radioactive analysis. We also want to extend a thank you to Adam Catasus and Ilexxis Morales for their help with the sample collection.

Supplementary materials

Supplementary material associated with this article can be found, in the online version, at doi:10.1016/j.hal.2022.102222.

References

Adhikari, P.L., Maiti, K., Overton, E.B., Rosenheim, B.E., Marx, B.D., 2016. Distributions and accumulation rates of polycyclic aromatic hydrocarbons in the northern Gulf of Mexico sediments. Environ. Pollut. 212, 413–423. https://doi.org/10.1016/j.envpol.2016.01.064.

Anderson, D.M., Hoagland, P., Kaoru, Y., White, A W, 2000. Estimated Annual Economic Impacts from Harmful Algal Blooms (HABs) in the United States. Woods Hole Oceanographic Institution, Woods Hole, MA. https://doi.org/10.1575/1912/96.

Appleby, P.G., Oldfield, F., 1978. The calculation of lead-210 dates assuming a constant rate of supply of unsupported 210Pb to the sediment. CATENA 5, 1–8 https://doi.org/10.1016/S0341-8162(78)80002-2.

Backer, L.C., Kirkpatrick, B., Fleming, L.E., Cheng, Y.S., Pierce, R., Bean, J.A., Clark, R., Johnson, D., Wanner, A., Tamer, R., Zhou, Y., Baden, D.G., 2005. Occupational exposure to aerosolized brevetoxins during Florida red tide events: effects on a healthy worker population. Environ. Health Perspect. 113, 644–649. https://doi.org/10.1289/ehp.7502.

Baden, D.G., Bourdelais, A.J., Jacocks, H., Michelliza, S., Naar, J., 2005. Natural and derivative brevetoxins: historical background, multiplicity, and effects. Environ. Health Perspect. 113 (5), 621–625.

Baumard, P., Budzinski, H., Garrigues, P., Raoux, C., Bellocq, J., Thompson, S., 2001. Chapter 6 - comparative study of sediment and mussel aromatic compound content in European coastal environments. relationship with specific biomarkers. In: Garrigues, PHILIPPE, Barth, H., Walker, C.H., Narbonne, J.F. (Eds.), Biomarkers in Marine Organisms. Elsevier Science, Amsterdam, pp. 131–177. https://doi.org/10.1016/B978-044482913-9/50008-0.

Brand, L.E., Compton, A., 2007. Long-term increase in Karenia brevis abundance along the Southwest Florida Coast. Harmful Algae 6, 232–252. https://doi.org/10.1016/j.hal.2006.08.005.

CDC | Case Definition: Brevetoxin Poisoning [WWW Document], 2019. URL https://emergency.cdc.gov/agent/brevetoxin/casedef.asp (accessed 8.20.20).

Burns, J., 2008. Cyanobacterial Harmful Algal Blooms: State of the Science and Research Needs, Advances in Experimental Medicine and Biology. Springer, New York, New York, NY. https://doi.org/10.1007/978-0-387-75865-7.

Conley, Daniel J., Carstensen, J., Vaquer-Sunyer, R., Duarte, C.M., 2009. Ecosystem thresholds with hypoxia. In: Andersen, J.H., Conley, D.J. (Eds.), Eutrophication in Coastal Ecosystems: Towards Better Understanding and Management Strategies

Selected Papers from the Second International Symposium on Research and Management of Eutrophication in Coastal Ecosystems, 20–23 June 2006, Nyborg, Denmark. Developments in Hydrobiology. Springer Netherlands, Dordrecht, pp. 21–29. https://doi.org/10.1007/978-90-481-3385-7_3.

D'Silva, M.S., Anil, A.C., Borole, D.V., Nath, B.N., Singhal, R.K., 2012. Tracking the history of dinoflagellate cyst assemblages in sediments from the west coast of India. J. Sea Res. 73, 86–100. https://doi.org/10.1016/j.seares.2012.06.013.

De Souza, V.L., Rodrigues, K.R., Pedroza, E.H., Melo, R.T.D., Lima, V.L.D., Hazin, C.A., de Almeida, M.G., Nascimento, R.K.D., 2012. Sedimentation rate and 210 Pb sediment dating at Apipucos Reservoir, Recife, Brazil. Sustainability 4 (10), 2419–2429.

Dickey, T.D., Chang, G.C., Agrawal, Y.C., Williams, A.J., Hill, P.S., 1998. Sediment resuspension in the wakes of hurricanes Edouard and Hortense. Geophys. Res. Lett. 25, 3533–3536. https://doi.org/10.1029/98GL02635.

Domingo, M., Kennedy, S., van Bressem, M.-F., 2001. Marine Mammal Mass Mortalities. In: Evans, P.G.H., Raga, J.A. (Eds.), Marine Mammals: Biology and Conservation. Springer US, Boston, MA, pp. 425–456. https://doi.org/10.1007/978-1-4615-0529-7_12.

Donaghay, P.L., Osborn, T.R., 1997. Toward a theory of biological-physical control of harmful algal bloom dynamics and impacts. Limnol. Oceanogr. 42, 1283–1296. https://doi.org/10.4319/lo.1997.42.5_part_2.1283.

Dupont, J.M., Hallock, P., Jaap, W.C., 2010. Ecological impacts of the 2005 red tide on artificial reef epibenthic macroinvertebrate and fish communities in the eastern Gulf of Mexico. Mar. Ecol. Prog. Ser. 415, 189–200, 10.3354/meps08739.

FDEM, 2018. ESF-18 Business damage assessment statewide summary report. Southwest Florida Red Tide. Florida division of emergency management.

Feinstein, A., Ceurvels, A.R., Hutton, R.F., Snoek, E., Smith, F.W., 1955. Red tide outbreaks off the Florida west coast. RED 55, 15.

Figueiras, F.G., Pitcher, G.C., Estrada, M., 2006. Harmful Algal Bloom Dynamics in Relation to Physical Processes. Ecology of Harmful Algae 127–138. https://doi.org/10.1007/978-3-540-32210-8_10.

Flaherty, K.E., Landsberg, J.H., 2011. Effects of a persistent red tide (Karenia brevis) bloom on community structure and species-specific relative abundance of Nekton in a Gulf of Mexico Estuary. Estuaries Coasts 34, 417–439. https://doi.org/10.1007/s12237-010-9350-x.

Fleming Lora, E., Kirkpatrick, Barbara, Backer Lorraine, C., Bean Judy, A., Wanner, Adam, Dalpra, Dana, Tamer, Robert, Zaias, Julia, Cheng Yung, Sung, Pierce, Richard, Naar, Jerome, Abraham, William, Clark, Richard, Zhou, Yue, Henry Michael, S., Johnson, David, Van De Bogart, Gayl, Bossart Gregory, D., Harrington, Mark, G, B.D., 2005. Initial evaluation of the effects of aerosolized Florida red tide toxins (brevetoxins) in persons with asthma. Environ. Health Perspect. 113, 650–657. https://doi.org/10.1289/ehp.7500.

Fleming, L.E., Kirkpatrick, B., Backer, L.C., Bean, J.A., Wanner, A., Reich, A., Zaias, J., Cheng, Y.S., Pierce, R., Naar, J., Abraham, W.M., Baden, D.G., 2007. Aerosolized red-tide toxins (Brevetoxins) and asthma. Chest 131, 187–194. https://doi.org/10.1378/chest.06-1830.

Fleming, L.E., Kirkpatrick, B., Backer, L.C., Walsh, C.J., Nierenberg, K., Clark, J., Reich, A., Hollenbeck, J., Benson, J., Cheng, Y.S., Naar, J., Pierce, R., Bourdelais, A. J., Abraham, W.M., Kirkpatrick, G., Zaias, J., Wanner, A., Mendes, E., Shalat, S., Hoagland, P., Stephan, W., Bean, J., Watkins, S., Clarke, T., Byrne, M., Baden, D.G., 2011. Review of Florida red tide and human health effects. Harmful Algae 10, 224–233. https://doi.org/10.1016/j.hal.2010.08.006.

Florida Fish and Wildlife Conservation Commission (FWC), 2018. FLSTSSN Archived Sea Turtle Stranding Data. https://myfwc.com/research/wildlife/sea-turtles/mortality/archived-stranding-data/.

Florida Fish and Wildlife Conservation Commission (FWC). 2021. Red Tide Manatee Mortalities. https://myfwc.com/research/manatee/rescue-mortality-response/statistics/mortality/red-tide/.

Florida Fish and Wildlife Conservation Commission (FWC), 2020. Recent harmful algal bloom (HAB) events [WWW Document]. URL https:/g-1eodata.myfwc.com/datasets/recent-harmful-algal-bloom-hab-events/data?geometry=-90.300,24.646,-73.611,28.090 (accessed 1.3.21).

Gobler, C.J., Sañudo-Wilhelmy, S.A., 2003. Cycling of colloidal organic carbon and nitrogen during an estuarine phytoplankton bloom. Limnol. Oceanogr. 48, 2314–2320. https://doi.org/10.4319/lo.2003.48.6.2314.

Guerin, T.F., 1999. The extraction of aged polycyclic aromatic hydrocarbon (PAH) residues from a clay soil using sonication and a Soxhlet procedure: a comparative study. J. Environ. Monit. 1, 63–67. https://doi.org/10.1039/a807307d.

Guven, D.E., Akinci, G., 2013. Effect of sediment size on bioleaching of heavy metals from contaminated sediments of Izmir Inner Bay. Journal of Environmental Sciences 25, 1784–1794. https://doi.org/10.1016/S1001-0742(12)60198-3.

Hardman, R.C., Cooper, W.J., Bourdelais, A.J., Gardinali, P., Baden, D.G., 2004. Brevetoxin degradation and by-product formation via natural sunlight. harmful algae 2002. In: Proc. Xth Int. Conf. Harmful Algae St Pete Beach Fla. USA Oct. 21-25 2002 Ed. Karen Steidinger Int. Conf. Harmful Algae 10th 200, 10, pp. 153–154.

He, Q., Walling, D.E., 1996. Interpreting particle size effects in the adsorption of 137Cs and unsupported 210 Pb by mineral soils and sediments. J. Environ. Radioact. 30, 117–137. https://doi.org/10.1016/0265-931X(96)89275-7.

Heil, C.A., Dixon, L.K., Hall, E., Garrett, M., Lenes, J.M., O'Neil, J.M., Walsh, B.M., Bronk, D.A., Killberg-Thoreson, L., Hitchcock, G.L., Meyer, K.A., Mulholland, M.R., Procise, L., Kirkpatrick, G.J., Walsh, J.J., Weisberg, R.W., 2014. Blooms of Karenia brevis (Davis) G. Hansen & Ø. Moestrup on the West Florida Shelf: Nutrient sources and potential management strategies based on a multi-year regional study. Harmful Algae 38, 127–140. https://doi.org/10.1016/j.hal.2014.07.016.

Hobbs, W.O., Dreher, T.W., Davis, E.W., Vinebrooke, R.D., Wong, S., Weissman, T., Dawson, M., 2021. Using a lake sediment record to infer the long-term history of cyanobacteria and the recent rise of an anatoxin producing Dolichospermum sp. Harmful Algae 101, 101971. https://doi.org/10.1016/j.hal.2020.101971.

Hu, C., Muller-Karger, F.E., Swarzenski, P.W., 2006. Hurricanes, submarine groundwater discharge, and Florida's red tides. Geophysical Research Letters. https://doi.org/10.1029/2005GL025449.

Huisman, J., Oostveen, P., van F.J., Weissing, 1999. Critical depth and critical turbulence: two different mechanisms for the development of phytoplankton blooms. Limnol. Oceanogr. 44, 1781–1787. https://doi.org/10.4319/lo.1999.44.7.1781.

Ingersoll, E., 1881. In: On the fish-mortality in the Gulf of Mexico. Proc. U. S. Natl. Mus.

Ishida, H., Nozawa, A., Hamano, H., Naoki, H., Fujita, T., Kaspar, H.F., Tsuji, K., 2004. Brevetoxin B5, a new brevetoxin analog isolated from cockle Austrovenus stutchburyi in New Zealand, the marker for monitoring shellfish neurotoxicity. Tetrahedron Lett. 45, 29–33. https://doi.org/10.1016/j.tetlet.2003.10.124.

Jenkins, C., 2018. Sediment accumulation rates for the Mississippi delta region: a time-interval synthesis. J. Sediment. Res. 88, 301–309. https://doi.org/10.2110/jsr.2018.15.

Joyce, S., 2000. The dead zones: oxygen-starved coastal waters. Environ. Health Perspect. 108, A120–A125. https://doi.org/10.1289/ehp.108-a120.

Kennish, M.J., Bricker, S.B., Dennison, W.C., Glibert, P.M., Livingston, R.J., Moore, K.A., Noble, R.T., Paerl, H.W., Ramstack, J.M., Seitzinger, S., Tomasko, D.A., Valiela, I., 2007. Barnegat bay–little egg harbor estuary: case study of a highly eutrophic coastal bay system. Ecol. Appl. 17, S3–S16. https://doi.org/10.1890/05-0800.1.

Kieber, R.J., Pitt, J., Skrabal, S.A., Wright, J.L.C., 2010. Photodegradation of the brevetoxin PbTx-2 in coastal seawater. Limnol. Oceanogr. 55, 2299–2304. https://doi.org/10.4319/lo.2010.55.6.2299.

Kirkpatrick, B., Fleming, L.E., Backer, L.C., Bean, J.A., Tamer, R., Kirkpatrick, G., Kane, T., Wanner, A., Dalpra, D., Reich, A., Baden, D.G., 2006. Environmental exposures to Florida red tides: effects on emergency room respiratory diagnoses admissions. Harmful Algae 5, 526–533. https://doi.org/10.1016/j.hal.2005.09.004.

Macrotrends, 2021. Florida Population 1900-2020 [WWW Document]. URL https://www.macrotrends.net/states/florida/population (accessed 5.19.21).

Kusek, K.M., Vargo, G., Steidinger, K.A., 1999. Gymnodinium breve in the field, in the lab, and in the newspaper- a scientific and journalistic analysis of Florida red tides. Contributions in marine science.

Liu, Y., Zhang, P., Du, S., Lin, Z., Zhou, Y., Chen, L., Yu, R., Zhang, L., 2019. Sediment as a Potential Pool for Lipophilic Marine Phycotoxins with the Case Study of Daya Bay of China. Mar Drugs 17, 623. https://doi.org/10.3390/md17110623.

Lubis, A.A., 2006. Constant rate of supply (CRS) model for determining the sediment accumulation rate in the coastal area using 210Pb. J Coast Dev 10.

Magaña, H.A., Contreras, C., Villareal, T.A., 2003. A historical assessment of Karenia brevis in the western Gulf of Mexico. Harmful Algae 2, 163–171. https://doi.org/10.1016/S1568-9883(03)00026-X.

Martin, T., Muller, J., 2021. The geologic record of Hurricane Irma in a Southwest Florida back-barrier lagoon. Mar. Geol. 441, p.106635.

Mendoza, W.G., Mead, R.N., Brand, L.E., Shea, D., 2008. Determination of brevetoxin in recent marine sediments. Chemosphere 73, 1373–1377. https://doi.org/10.1016/j.chemosphere.2008.07.089.

Morgan, K.L., Larkin, S.L., Adams, C.M., 2007. Public Costs of Florida Red Tides 2007, 4.

Nakanishi, K., 1985. The chemistry of brevetoxins: a review. Toxicon 23, 473–479. https://doi.org/10.1016/0041-0101(85)90031-5.

Ott, J.A., Duffey, R.M., Erickson, S.E., Fuhr, K.S., Rodgers, B.A., Schneider, M.A., 2006. Comparison of light limiting water quality factors in six Florida aquatic preserves. Fla. Sci. 69, 73–91.

Paerl, H.W., Barnard, M.A., 2020. Mitigating the global expansion of harmful cyanobacterial blooms: moving targets in a human- and climatically-altered world. Harmful Algae 96, 101845. https://doi.org/10.1016/j.hal.2020.101845.

Parsons, M.L., Dortch, Q., Turner, R.E., 2002. Sedimentological evidence of an increase in Pseudo-nitzschia (Bacillariophyceae) abundance in response to coastal eutrophication. Limnol. Oceanogr. 47, 551–558.

Perkins, S., 2019. Inner workings: ramping up the fight against Florida's red tides. Proc. Natl. Acad. Sci 116, 6510–6512. https://doi.org/10.1073/pnas.1902219116.

Pierce, R., Henry, M., Blum, P., 2007. Brevetoxin abundance and composition during ECOHAB-Florida field monitoring cruises in the Gulf of Mexico. Cont. Shelf Res. 28, 45–58. https://doi.org/10.1016/j.csr.2007.04.012.

Pierce, R.H., Henry, M.S., Blum, P.C., Hamel, S.L., Kirkpatrick, B., Cheng, Y.S., Zhou, Y., Irvin, C.M., Naar, J., Weidner, A., Fleming, L.E., Backer, L.C., Baden, D.G., 2005. Brevetoxin composition in water and marine aerosol along a Florida beach: assessing potential human exposure to marine biotoxins. Harmful Algae 4, 965–972. https://doi.org/10.1016/j.hal.2004.11.004.

Pierce, R.H., Henry, M.S., Blum, P.C., Lyons, J., Cheng, Y.S., Yazzie, D., Zhou, Y., 2003. Brevetoxin concentrations in marine aerosol: human exposure levels during a Karenia brevis harmful algal bloom. Bull. Environ. Contam. Toxicol. 70, 161–165. https://doi.org/10.1007/s00128-002-0170-y.

Pitt, J., 2007. Photochemistry of brevetoxin, PbTx-2, produced by the dinoflagellate Karenia brevis 50.

Poli, M.A., Musser, S.M., Dickey, R.W., Eilers, P.P., Hall, S., 2000. Neurotoxic shellfish poisoning and brevetoxin metabolites: a case study from Florida. Toxicon 38, 981–993. https://doi.org/10.1016/S0041-0101(99)00191-9Savarese, M., Loh, A.N. and Trefry, J.H., 2004. Environmental and hydrologic history of Estero Bay: implications for watershed management and restoration. South Florida Water Management District, Technical Report, p.76.

Schumacher, B.A., 2002. Methods for the determination of total organic carbon (TOC) in soils and sediments 25.

Pierce, R., Henry, M., Blum, P., Payne, S.. Gymnodinium breve toxins without cells: intra-cellular and extra-cellular toxins. Harmful algal blooms 421–424. ScienceDirect. https://doi.org/10.1006/ecss.1999.0516.

Pierce, RH., Henry, MS., Proffitt, LS., Hasbrouck, P., 1990. Red tide toxin (brevetoxin) enrichment in marine aerosol. Toxic Marine Phytoplankton 397–402.
Roberts, D., 2012. Causes and ecological effects of resuspended contaminated sediments (RCS) in marine environments. Environment international 40, 230–243. https://doi.org/10.1016/j.envint.2011.11.013.
Shea, D., 1997. Analysis of brevetoxins by micellar electrokinetic capillary chromatography and laser-induced fluorescence detection. Electrophoresis 18, 277–283. https://doi.org/10.1002/elps.1150180216.
Singleton, A.A., Schmidt, A.H., Bierman, P.R., Rood, D.H., Neilson, T.B., Greene, E.S., Bower, J.A., Perdrial, N., 2017. Effects of grain size, mineralogy, and acid-extractable grain coatings on the distribution of the fallout radionuclides 7Be, 10Be, 137Cs, and 210 Pb in river sediment. Geochim. Cosmochim. Acta 197, 71–86. https://doi.org/10.1016/j.gca.2016.10.007.
US Department of Commerce, N.O. and A.A., n.d. Florida: Harmful Algal Blooms [WWW Document]. URL https://oceanservice.noaa.gov/hazards/hab/florida-2018.html (accessed 8.20.20). 2019.
Xu, H., Paerl, H.W., Qin, B., Zhu, G., Gaoa, G., 2010. Nitrogen and phosphorus inputs control phytoplankton growth in eutrophic Lake Taihu. China. Limnol. Oceanogr. 55, 420–432. https://doi.org/10.4319/lo.2010.55.1.0420.
Xu, K., Mickey, R.C., Chen, Q., Harris, C.K., Hetland, R.D., Hu, K., Wang, J., 2016. Shelf sediment transport during hurricanes Katrina and Rita. Comput. Geosci., Uncertainty and Sensitivity in Surface Dynamics Modeling 90, 24–39. https://doi.org/10.1016/j.cageo.2015.10.009.
Zastepa, A., Taranu, Z.E., Kimpe, L.E., Blais, J.M., Gregory-Eaves, I., Zurawell, R.W., Pick, F.R., 2017. Reconstructing a long-term record of microcystins from the analysis of lake sediments. Sci. Total Environ. 579, 893–901. https://doi.org/10.1016/j.scitotenv.2016.10.211.
Court, C., Ferreira, J., Ropicki, A., Qiao, X., Bijeta, S., 2021. Quantifying the Socio-Economic Impacts of Harmful Algal Blooms in Southwest Florida in 2018 1–50.
Latimer, J. S., Davis, W. R., & Keith, D. J. (1999). Mobilization of PAHs and PCBs from In-Place Contaminated Marine Sediments During Simulated Resuspension Events.
Savarese, M., Loh, A.N., Trefry, J., 2004. Environmental and Hydrologic History of Estero Bay: Implications for Watershed Management and Restoration. 2006 South Florida Environmental Report 132.
Rounsefell, G.A., Nelson, W.R., 1966. Red-tide Research Summarized to 1964. Including an Annotated Bibliography.